Matsubayashi et al., http://www.jcb.org/cgi/content/full/jcb.201411037/DC1

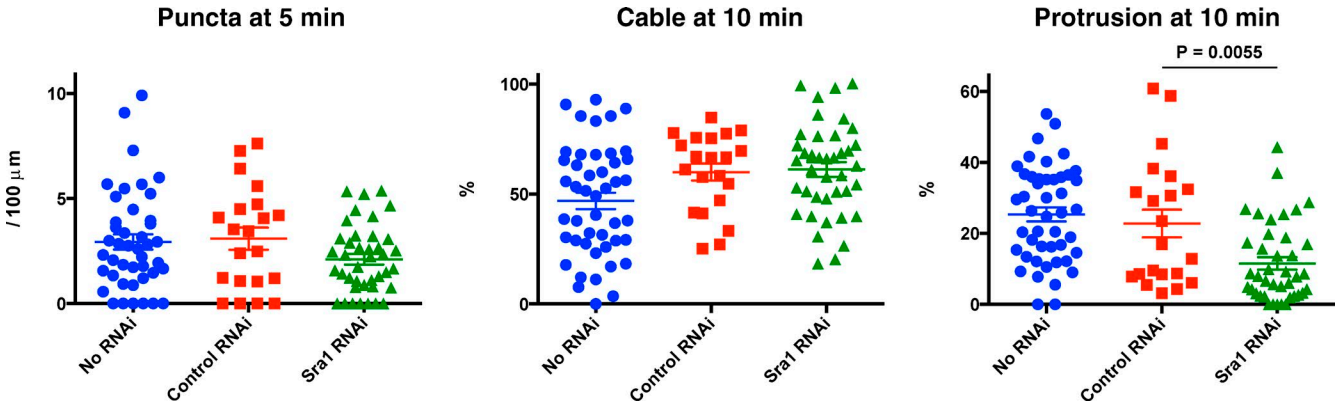

Figure S1. **RNAi-mediated knockdown of *sra1*, a gene encoding a regulatory subunit of the SCAR complex, produces results consistent with those obtained for *SCAR*$^{\Delta 37}$ mutants.** Quantification of the formation of actin puncta, cable, and protrusions during wound healing in embryos expressing no RNAi, a control RNAi against *ebony*, or an RNAi against *sra1* (which encodes a regulatory subunit of the SCAR complex) under the control of TubP-Gal4. F-actin was visualized using GFP-Moesin. Bars indicate the means ± SEM of all plotted values.

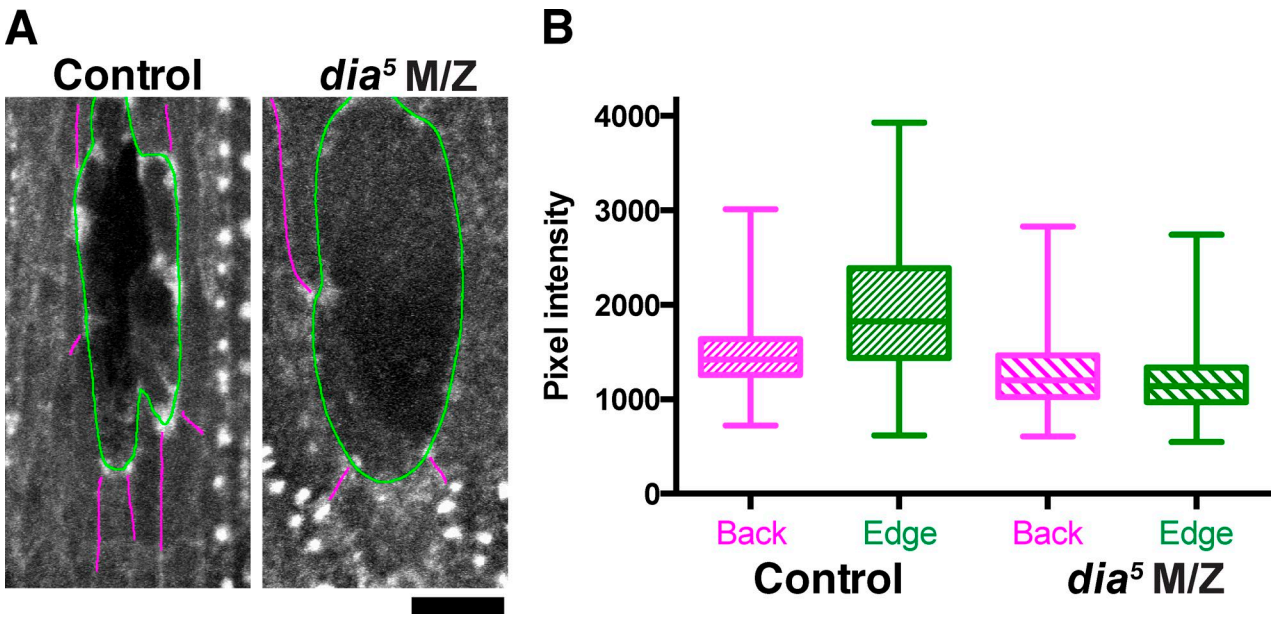

Figure S2. **Quantification of the fluorescence intensity of wound edge F-actin and cortical actin behind the edge in control and *dia*^{5} M/Z embryos.** Quantification of the fluorescence intensity of wound edge F-actin (traced by green line in A and labeled Edge in B) and cortical F-actin just behind the wound edge (traced by magenta line in A and labeled Back in B) in the 4-min images displayed in Fig. 3 A. The distribution of the pixel intensity on the green and magenta lines in each image is shown in B. The boxes extend from the 25 to 75 percentiles, and the whiskers extend from the minimum to maximum. The bars in the middle of the boxes indicate the median. Note that the intensity of Edge actin is significantly greater than Back in control embryos ($P < 0.0001$), whereas in *dia*^{5} M/Z embryos, the Edge intensity is no greater than Back.

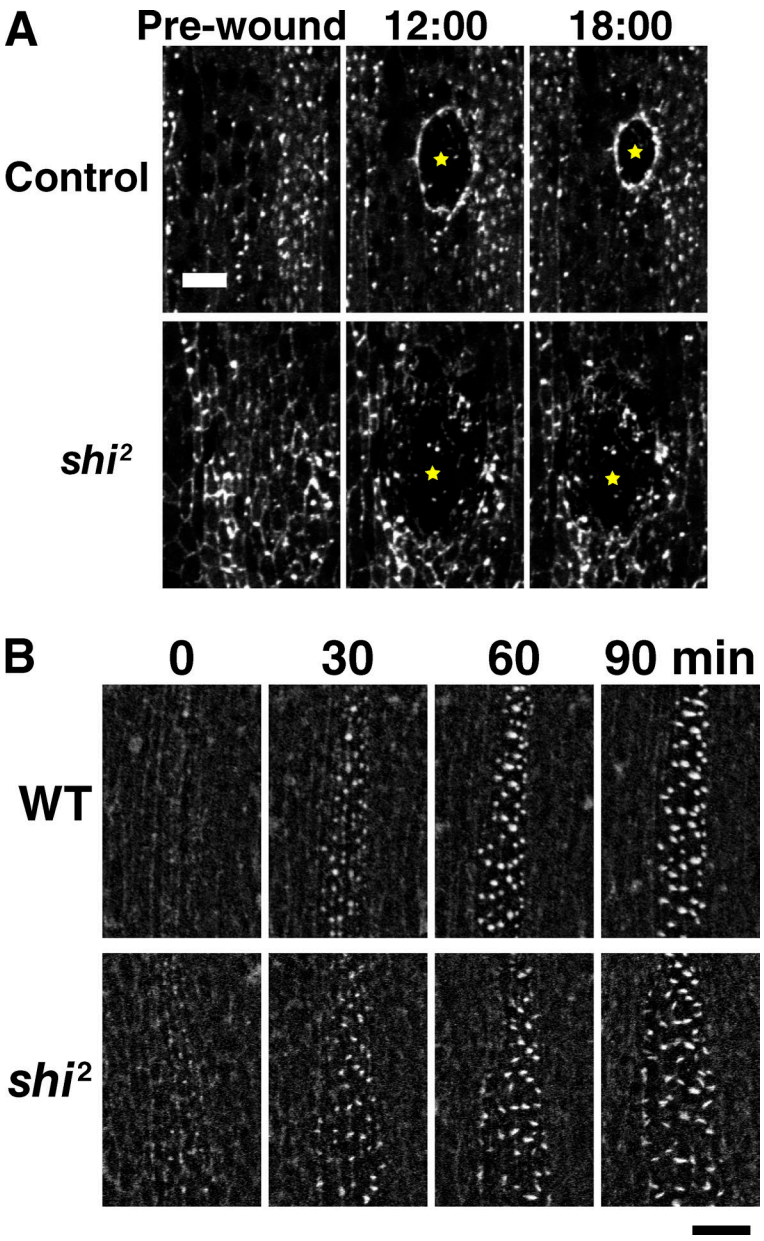

Figure S3. **GFP-Zipper distribution and denticle development in control or *shi²* embryos.** Experiments performed at 30°C. (A) GFP-Zipper accumulates at the wound edge in control embryos (top) but not *shi²* embryos. Time points indicate time after wounding (minutes and seconds). Stars indicate the position of the wounds. Bar, 10 µm. (B) The ventral epidermis of control and *shi²* embryos expressing GFP-Moesin. Note that denticle development is not perturbed in *shi²* embryos. Images recorded at indicated time points after start of experiment. WT, wild type. Bar, 20 µm.

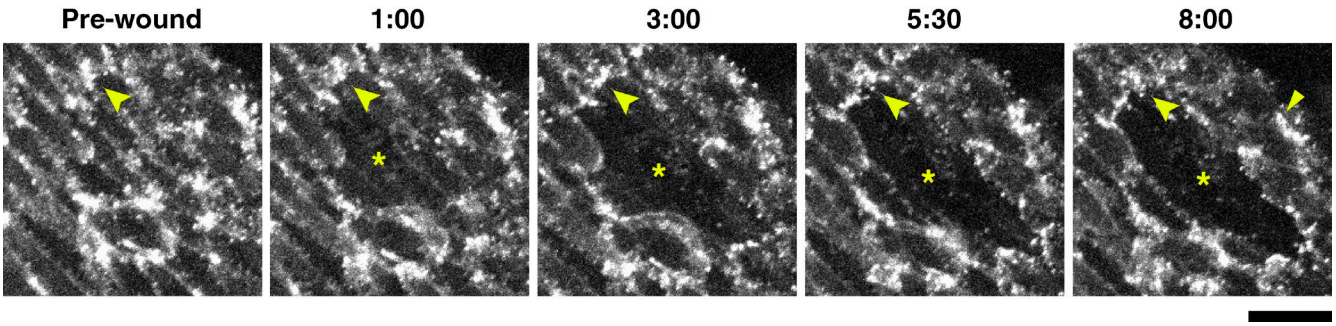

Figure S4. **Localization of GFP-DiaΔDAD during wound healing.** Time points after wounding are indicated (minutes and seconds). Levels of GFP-DiaΔDAD at wound edge junctions after wounding are comparable to that at the equivalent TCJ before wounding (large arrowheads, all images) and that at other TCJs behind the wound edge (small arrowhead, right-hand image). Asterisks indicate center of wound. Bar, 10 µm.

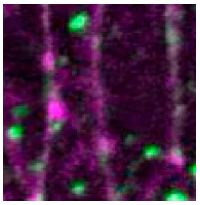

Video 1. **Dynamics of actin and myosin at the wound edge.** Images from this video are displayed in Fig. 1 D. The epidermis of a *Drosophila* embryo expressing mCherry-Moesin (magenta) and GFP-Zipper (green) was wounded and subjected to time-lapse live imaging. Merged images were also shown. The time after wounding is indicated (minutes and seconds). The size of the imaged area is 12 µm × 12 µm.

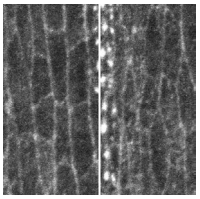

Video 2. **Dynamics of actin during wound healing in control and *SCAR*$^{\Delta 37}$ embryos.** Images from this video are displayed in Fig. 2 A. *Drosophila* embryos expressing GFP-Moesin (left, control; right, *SCAR*$^{\Delta 37}$ zygotic mutant) were wounded and subjected to time-lapse live imaging. The time after wounding is indicated (minutes and seconds). The size of the imaged areas is 20 µm × 40 µm.

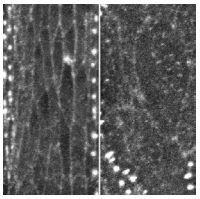

Video 3. **Dynamics of actin during wound healing in control and *dia*^{5} M/Z embryos.** Images from this video are displayed in Fig. 3 A. *Drosophila* embryos expressing GFP-Moesin (left, control; right, *dia*^{5} M/Z mutant) were wounded and subjected to time-lapse live imaging. The time after wounding is indicated (minutes and seconds). The size of the imaged areas is 26.7 µm × 53.4 µm.

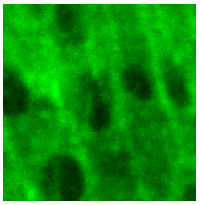

Video 4. **Dynamics of actin and Dynamin during wound healing.** Images from this video are displayed in Fig. 5 A. *Drosophila* embryos expressing Dynamin-GFP (green) and mCherry-Moesin (magenta) were wounded and subjected to time-lapse live imaging. Individual channels and a merged image are shown. The time after wounding is indicated (minutes and seconds). The size of the imaged areas is 20 µm × 20 µm.

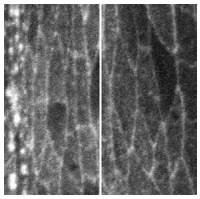

Video 5. **Dynamics of actin during wound healing in control and *shi*^{2} embryos.** *Drosophila* embryos expressing GFP-Moesin (left, control; right, *shi*^{2} mutant) were wounded and subjected to time-lapse live imaging. The time after wounding is indicated (minutes and seconds). The images at 2 min and 30 s in this video are displayed in Fig. 5 E (top right). The size of the imaged areas is 20 µm × 40 µm.

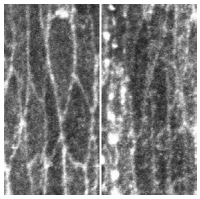

Video 6. **Dynamics of actin during wound healing in control and Rab5DN-expressing embryos.** *Drosophila* embryos expressing GFP-Moesin ± Rab5-DN (left, control; right, +Rab5DN) were wounded and subjected to time-lapse live imaging. The time after wounding is indicated (minutes and seconds). The images at 2 min and 30 s in this video are displayed in Fig. 5 E (bottom right). The size of the imaged areas is 20 µm × 40 µm.

Table S1. **Genotypes of the embryos used in each experiment**

Figure	Panel	Genotype
Fig. 1	A	e22c-Gal4, UAS-GMA/+
	B	e22c-Gal4, UAS-mCherry-Moesin, Ubi-DEcad-GFP/+
	D	e22c-Gal4, UAS-mCherry-Moesin, UAS-GFP-Zipper/+; i76D-Gal4, UAS-mCherry-Moesin/+
	E	112A-Gal4, cGMA
	F, left	112A-Gal4, cGMA
	F, middle and right	e22c-Gal4, UAS-GMA/+
Fig. 2	A–C, Control	112A-Gal4, cGMA
	A–C, $SCAR^{\Delta 37}$	112A-Gal4, cGMA; $SCAR^{\Delta 37}$
Fig. 3	A–D, Control	112A-Gal4, cGMA
	A and B, dia^5 M/Z	112A-Gal4, cGMA; dia^5 M/Z[a]
	D, $dia^{5\,M}$/Df	112A-Gal4, cGMA; $dia^{5\,M}$/Df
	E, Control	Df(2L)ED1317, sqh-GFP/+
	E, $dia^{5\,M}$/Df	Df(2L)ED1317, sqh-GFP/dia^5
Fig. 4	Control	cGMA
	WASp^3	cGMA; e^1, $WASp^3$
Fig. 5	A	e22c-Gal4, UAS-mCherry-Moesin, UAS-Dyn-GFP/+
	B and C, Control	e22c-Gal4, UAS-mCherry-Moesin/+
	B and C, shi^2	shi^2; e22c-Gal4, UAS-mCherry-Moesin/+
	B and C, shi^2 + Dyn-GFP	shi^2; e22c-Gal4, UAS-mCherry-Moesin/UAS-Dyn-GFP
	D, top, Control	e22c-Gal4, UAS-mCherry-Moesin/UAS-CLC-GFP
	D, bottom, shi^2	shi^2; e22c-Gal4, UAS-mCherry-Moesin/UAS-CLC-GFP
	E, top, shi^2	shi^2; e22c-Gal4, UAS-GMA/+
	E, bottom, Control	e22c-Gal4, UAS-GMA/+, UAS-RedStinger/+[b]
	E, bottom, Rab5DN	e22c-Gal4, UAS-GMA/+, UAS-Rab5DN/+
	F, Control	e22c-Gal4, UAS-GMA/+
	F, Rab5DN	e22c-Gal4, UAS-GMA/+, UAS-Rab5DN/+
Fig. 6	A–D, GFP-Dia, Control	e22c-Gal4, UAS-mCherry-Moesin/UAS-GFP-Dia
	A–D, GFP-Dia, shi^2	shi^2; e22c-Gal4, UAS-mCherry-Moesin/UAS-GFP-Dia
	A, GFP	e22c-Gal4, UAS-mCherry-Moesin/+; i76D-Gal4, UAS-mCherry-Moesin/UAS-GFP
Fig. 7	A and B, Control	e22c-Gal4, UAS-mCherry-Moesin, Ubi-DEcad-GFP/+
	A and B, Rab5DN	e22c-Gal4, UAS-mCherry-Moesin, Ubi-DEcad-GFP/+; UAS-Rab5DN/+
	C and D, Control	112A-Gal4, cGMA
	C and D, shg^{k03401}	112A-Gal4, cGMA; shg^{k03401}
	E, Control	112A-Gal4, cGMA
	E, shg^{k03401}/+	112A-Gal4, cGMA; shg^{k03401}/+
	E, shi^2	112A-Gal4, cGMA, shi^2
	E, shi^2; shg^{k03401}/+	112A-Gal4, cGMA, shi^2; shg^{k03401}/+
	F, Control	112A-Gal4, cGMA
	F, p120def	112A-Gal4, cGMA; p120ctn deficient[c]
	F, shi^2	112A-Gal4, cGMA, shi^2
	F, shi^2; p120def	112A-Gal4, cGMA, shi^2; p120ctn-deficient
Fig. S1	No RNAi	TubP-Gal4, UAS-GMA/+
	Control RNAi	TubP-Gal4, UAS-GMA/UAS-*ebony* RNAi
	Sra1 RNAi	TubP-Gal4, UAS-GMA/UAS-*sra1* RNAi
Fig. S2	Control	112A-Gal4, cGMA
	dia^5 M/Z	112A-Gal4, cGMA; dia^5 M/Z
Fig. S3	A, Control	e22c-Gal4, UAS-GFP-Zipper/+
	A, shi^2	shi^2; e22c-Gal4, UAS-GFP-Zipper/+
	B, Control	cGMA
	B, shi^2	cGMA, shi^2
Fig. S4	GFP-DiaΔDAD	e22c-Gal4, UAS-mCherry-Moesin, UAS-GFP-DiaΔDAD/+

cGMA, constitutive GFP-Moesin; CLC, clathrin light chain; DE-cad, *Drosophila* E-cadherin; GMA, GFP-Moesin; Ubi, ubiquitin promoter.
[a]For details of *dia* mutants, see Materials and methods.
[b]RedStinger is a DsRed RFP targeted to the nucleus. It was used as a control.
[c]For details of p120def, see Materials and methods.